ISBN: 978-3-95450-219-6 ISSN: 2226-0366 doi: 10.18429/JACoW-LINAC2024-THPB101

LONGITUDINAL BEAM DYNAMICS OPTIMIZATION FOR INFRARED TERAHERTZ FEL LINAC

Y. M. Yang, S. C. Zhang, Z. G. He, G. Y. Feng†
University of Science and Technology of China, Hefei, China

Abstract

The high-repetition-rate infrared terahertz free-electron laser (IR-THz FEL) facility is progressing in the preliminary research stage, which can achieve the demand for a tunable high-power light source in the long wavelength spectrum and form a complementary structure of advantages with the Hefei Advanced Light Facility (HALF). In this paper, we present the design of a bunch compressor, enabling compress the bunch length to reach the peak current of 118 A. We also introduce an approach to optimize the RF parameters for the accelerating modules, which makes it feasible to generate a high-quality beam bunch that can reach the requirements for future FEL applications.

INTRODUCTION

The paper introduces the design and optimization of a high-repetition-rate IR-THz FEL facility [1–4], which leverages optical resonator-based FEL technology to achieve a higher mean power output by increasing pulse frequency. Electron beam of the facility will be generated from a photocathode RF gun injector and further accelerated with a superconducting linear accelerator. The C-type bending magnet chicane is used to increase the peak current by compressing the bunch length. During the beam dynamics simulations, space charge effects, coherent synchrotron radiation (CSR) effects and longitudinal cavity wake field effects have been taken into account with the codes of ASTRA [5] and CSRTrack [6].

LAYOUT

The schematic layout of the IR-THz FEL facility is shown in Fig. 1. The injector consists of a photocathode RF gun, an L-band accelerating section and a third-harmonic accelerating section. The electron bunches are generated by using a normal conducting 1.3 GHz RF gun. reaching 5 MeV [7-8]. After the gun, the electron bunches are accelerated in a superconducting 9-cell TESLA cavity [9] with resonant frequency of 1.3 GHz: ACC1. Downstream of the ACC1 section, a third-harmonic RF system [10,11], operating at 3.9 GHz and referred to as ACC39, will be used to linearize the longitudinal phase space distribution with RF curvature distortion and to minimize the bunch tails in the subsequent chicane. The electron beam energy is 20 MeV at the exit of ACC39 section. There is a bunch compressor chicane (BC) with a C-type structure downstream of the ACC39 section. The beam energy is increased to 58 MeV after passing through the main linac, which is equipped with two L-band superconducting 9-cell TESLA cavities, named ACC2.

The IR-THz FEL will operate in the oscillator mode, which generates FEL radiation with wavelengths ranging from 5 μm to 1000 μm. After the ACC1 section, electron bunches are deflected to the undulator (U1) by a beam distribution system, and THz radiation with wavelength range of 200–1000 μm can be generated in the U1. Following the ACC2 section, the electron bunches are distributed into two distinct undulators, which generate mid-infrared (5–40 μm) and far-infrared (40–200 μm) radiation respectively.

BUNCH COMPRESSION

The linac-based free-electron laser require very short bunches of high-brightness electron beams with high peak currents. The bunches cannot be directly generated in rf-gun, as space charge forces would result in the deterioration of the beam quality in a short distance. Therefore, electron bunches must start with a low intensity and a few tens of Amperes peak current, and subsequently be accelerated to energy where the space charge effects are sufficiently weakened. In this case, the peak current can be increased by compressing the bunch length.

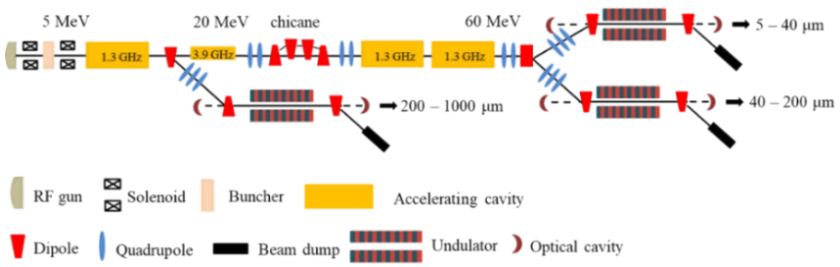

Figure 1: The schematic layout of the IR-THz FEL facility.

* Work supported by Supported by the Hundred-person Program of Chinese Academy of Sciences
† fenggy@ustc.edu.cn

ISBN: 978-3-95450-219-6 ISSN: 2226-0366 doi: 10.18429/JACoW-LINAC2024-THPB101

Table 1: Parameters for the Chicane

Parameter	Symbol	Value	Unit
Bend magnet length	L_B	0.1	m
Drift length B1-B2 and B3-B4	ΔL	0.15	m
Drift length B2-B3	ΔL_C	0.1	m
Bend radius of each dipole magnet	ρ	0.46	m
Bending angle	θ_0	12.6	deg
Momentum compaction	R_{56}	–22.1	mm
Total length of chicane	L_T	0.8	m
Bunch charge	q	0.5	nC
Electron energy	E	20	MeV
Compression factor	C	4.5	/

The usual technique starts out by introducing a correlation between the longitudinal position of the particles in and their energy using a RF accelerating system [12]. For a bending magnet chicane, the particle energy in the head of the bunch is reduced, while that in the tail is increased.

Lower-momentum particles reach the chicane first, but travel a longer distance than later, higher-momentum particles, a process known as 'ballistic bunching'. Figure 2 and Table 1 presents our C-type bending-magnet chicane [12–14].

Figure 2: C-type bending magnet chicane.

The non-linearities of both the accelerating RF fields and the longitudinal dispersion distorts the longitudinal phase space, shown in Fig. 3. The non-linearity of the fundamental RF frequency is already visible before compression as a curvature in the energy chirp (left plots). After compression, the non-linearity of the chirp, together with the T_{566} of the chicane, dominates the shape of the bunch in phase space. A sharp spike develops at the head of the charge distribution with a width depending on the intrinsic energy spread (center plots).

A higher-harmonic RF system can be used to compensate the non-linearities (right plots). In this case, the RF phase is set to the decelerating crest to compensate the 2nd-order curvature with a reasonable peak voltage.

BEAM DYNAMICS SIMULATION

In order to obtain FEL radiation with a short gain length, beam bunches require a high peak current, a small slice emittance, and a low energy spread at the entrance of the undulator section [15–16]. In the beam dynamics simulation, the peak current reach 118 A and the beam energy is 58 MeV after the main linac. The beam energy before the BC section is fixed as E_1 = 20 MeV.

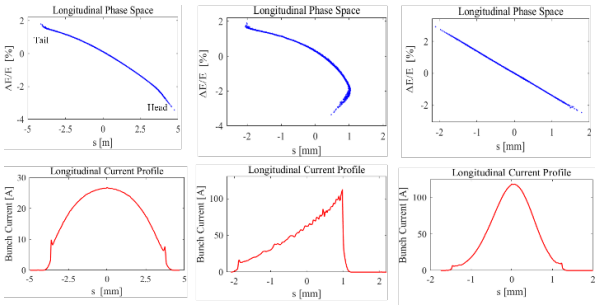

Figure 3: Longitudinal phase space and bunch current distribution before (left two plots) and after (center two plots) a bunch compressor chicane, and with 3rd-harmonic compensation.

The transformation of the longitudinal coordinate in the i^{th} bunch compressor is described by:

$$s_i = s_{i-1} - (R_{56i} \cdot \delta_i + T_{566i} \cdot \delta_i^2 + U_{5666i} \cdot \delta_i^3) \ ,$$

where R_{56i}, T_{566i} and U_{5666i} are the momentum compaction factors in the i^{th} compressor, and δ_i is the relative energy deviation. For the fixed values of RF parameters and momentum compaction factors, the global compression function can be defined as follows:

$$C_N = 1/Z_N \quad , \quad Z_N = \partial s_N / \partial s \ ,$$

where the function $C_N(s)$ describes the increase of the peak current in the slice with initial position s and $Z_N(s)$ is the inverse global compression function.

When collective effects are excluded in a one-stage bunch compression scheme, it is feasible to establish the relationship among the RF parameters, beam energies, and inverse global compression functions:

$$E_1 = E_1(V_1, \varphi_1, V_{39}, \varphi_{39})$$

$$Z_1 = \frac{\partial^2 s_1}{\partial s^2}(0) \ , \qquad Z_1' = \frac{\partial^2 s_1}{\partial s^2}(0), \qquad Z_1'' = \frac{\partial^3 s_1}{\partial s^3}(0) \ .$$

ISBN: 978-3-95450-219-6 ISSN: 2226-0366 doi: 10.18429/JACoW-LINAC2024-THPB101

The partial compression function $C_1 = 1/Z_1$ describes the amount of the compression achieved after the compressor. Z_1' can decide the symmetry of the current profile, while Z_1'' can decide the full width at half maximum (FWHM) value of the bunch length [17]. Figure 4 shows a comparative analysis that elucidates the impact of varying Z_1' and Z_1'' settings on both the current profiles and the longitudinal phase space.

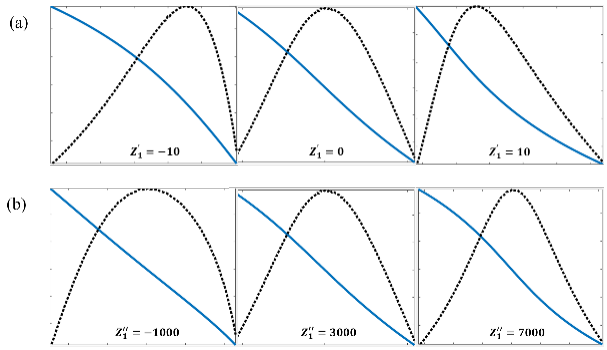

Figure 4: (a) Fixed $Z_1'' = 3000$, the current profile for the varied values of Z_1'. (b) Fixed $Z_1' = 0$, the FWHM value of the bunch length for the varied values Z_1''. Longitudinal phase space (bule lines), current profile (black lines).

In alignment with the theories previously articulated, we have developed the MATLAB-based code aimed at optimizing current profiles and longitudinal phase space. By manipulating the parameters $E_1, Z_1, Z_1' \, and \, Z_1''$, it becomes feasible to generate a beam bunch characterized by a specified beam energy, requisite peak current, and superior current profiles.

As an example, a 0.5-nC bunch ha an initial current of 26 A and a compression factor C1 equal to 4.5. A chicane of 12.6-degree bending angle provides 0.46-m bending radius, as in Table 1.

Vectors $\overrightarrow{x_0}$ and $\overrightarrow{f_0}$ are defined as follows:

$$\overrightarrow{x_0} = (V_1, \varphi_1, V_{39}, \varphi_{39})^{-1} \quad , \qquad \overrightarrow{f_0} = (E_1, Z_1, Z_1', Z_1'')^{-1}.$$

The relation between $\overrightarrow{x_0}$ and $\overrightarrow{f_0}$ can be written by using a nonlinear operator A_0: $\overrightarrow{f_0} = A_0(\overrightarrow{x_0})$. When the beam energies and the global compression functions are fixed, the RF parameters can be obtained by using $\overrightarrow{x_0} = A_0^{-1}(\overrightarrow{f_0})$. The RF parameter settings for the accelerating modules are shown in Table 2.

The beam dynamics simulation from the RF gun to the entrance of the undulator has been done with 10^5 particles. For all of the arc sections, CSRTrack code is used to take into account the CSR impact. The beam tracking in the straight sections is simulated with ASTRA code. Longitudinal cavity wake field effects are considered at the exit of each accelerating section with MATLAB scripts.

Table 2: RF Parameters for the Accelerating Modules

Parameter	Value	Unit
Charge Q	0.5	nC
V_{ACC1}	21.42	MV
φ_{ACC1}	15.59	deg
V_{ACC39}	6.40	MV
φ_{ACC39}	151.61	deg
V_{ACC2}	40	MV
φ_{ACC2}	0	deg

The beam bunch data is summarized as featuring a beam energy of 58.42 MeV, peak current of 118 A, projected emittances in the x-direction (ε_x) of 0.388 μm and in the y-direction (ε_y) of 0.688 μm, and a slice energy spread (σ_{max}) of 5.8 keV. Beam bunch properties at the entrance of the undulator section are shown in Fig. 5. The beam quality can reach the requirements for future FEL applications.

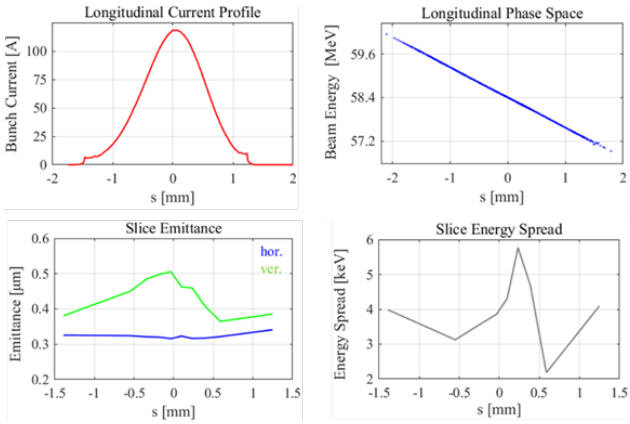

Figure 5: Beam bunch properties at the entrance of the undulator section: longitudinal phase space (top left), current profile (top right), slice emittances (bottom left), and slice energy spread (bottom right).

CONCLUSION

In this paper, the beam dynamics simulation for the high-repetition-rate IR-THz FEL facility is introduced which includes the parameters selection for the bunch compressor and the RF parameters calculation for the accelerating modules, while the collective effects are taken into account. To optimize current profiles and the longitudinal phase space, we have developed a MATLAB-based code. Consequently, it becomes feasible to generate a high-quality beam bunch that can reach the requirements for future FEL applications.

ISBN: 978-3-95450-219-6 ISSN: 2226-0366 doi: 10.18429/JACoW-LINAC2024-THPB101

REFERENCES

[1] G. Paraskaki *et al*., "High repetition rate seeded free electron laser with an optical klystron in high-gain harmonic generation", *Phys. Rev. Accel. Beams*, vol. 24, no. 12, pp. 120701, Dec. 2021. doi:10.1103/PhysRevAccelBeams.24.120701

[2] S. Ackermann *et al*., "Novel method for the generation of stable radiation from free-electron lasers at high repetition rates", *Phys. Rev. Accel. Beams*, vol. 23, no. 7, pp. 071302, Jul. 2020. doi:10.1103/PhysRevAccelBeams.23.071302

[3] H. Sun *et al*., "Seeding with a harmonic optical klystron resonator configuration in a high repetition rate free electron laser", *Phys. Rev. Accel. Beams*, vol. 25, no. 6, pp. 060701, Jun. 2022. doi:10.1103/PhysRevAccelBeams.25.060701

[4] K. Zhou *et al*., "General design of infrared terahertz free-electron laser facility of Chinese Academy of Engineering Physics," *Chin. J. Lasers*, vol. 50, no. 17, pp. 1718001, Sep. 2023. doi:10.3788/CJL230786

[5] K. Floettmann, "ASTRA", DESY, Hamburg: https://www.desy.de/~mpyflo/

[6] M. Dohlus and T. Limberg, "CSRtrack: faster calculation of 3D CSR effects", in *Proc. of FEL'04,* Trieste, Italy, Sep. 2004, paper MOC085.

[7] H. Xu *et al*., "Development of an L-band photocathode RF gun at Tsinghua University", *Nucl. Instrum. Methods Phys. Res., Sect. A*, vol. 985, p. 164675, 2021. doi:10.1016/j.nima.2020.164675

[8] Y. Song *et al*., "Development of a 1.4-cell RF photocathode gun for single-shot MeV ultrafast electron diffraction devices with femtosecond resolution", *Nucl. Instrum. Methods Phys. Res., Sect. A*, vol. 1031, p. 166602, 2022. doi:10.1016/j.nima.2022.166602

[9] A. Halavanau *et al*., "Analysis and measurement of the transfer matrix of a 9-cell, 1.3-GHz superconducting cavity", *Phys. Rev. Accel. Beams*, vol. 20, no. 4, p. 120701, Apr. 2017. doi:10.1103/PhysRevAccelBeams.20.120701

[10] M. Dolus, "FLASH beam dynamics issues with 3rd harmonic system", presented at MAC meeting, DESY, Germany, 2009, unpublished.

[11] D. Alesini *et al*., "Longitudinal beam dynamics in the Frascati DAΦNE e^+e^- collider with a passive third harmonic cavity in the lengthening regime", *Phys. Rev. Accel. Beams*, vol. 6, no. 4, pp. 074401, Jul. 2003. doi:10.1103/PhysRevAccelBeams.6.074401

[12] W. Chou, "ICFA beam dynamics newsletter", no. 38, Dec. 2005. https://icfa-usa.jlab.org/archive/newsletter/icfa_bd_nl_38.pdf

[13] F. Zhou *et al*., "Experimental characterization of the transverse phase space of a 60-MeV electron beam through a compressor chicane", *Phys. Rev. Accel. Beams*, vol. 9, no. 11, p. 114201, Nov. 2006. doi:10.1103/PhysRevAccelBeams.9.114201

[14] D. Khan and T. O. Raubenheimer, "Novel bunch compressor chicane: The five-bend chicane", *Phys. Rev. Accel. Beams*, vol. 25, no. 9, p. 090701, Sep. 2020. doi:10.1103/PhysRevAccelBeams.25.090701

[15] G. Y. Feng *et al*., "Beam dynamics simulation for FLASH2 HGHG option", in *Proc. LINAC'14*, Geneva, Switzerland, Aug. 2014, paper TUPP020, pp. 471–474.

[16] G. Y. Feng *et al*., "Start-to-end simulation for FLASH2 HGHG Option", in *Proc. FEL'14*, Basel, Switzerland, Aug. 2014, paper MOP083, pp. 244–247.

[17] G. Y. Feng *et al*., "Beam dynamics simulations for European XFEL", DESY, Hamburg, Rep. TESLA-FEL2013-04. https://flash.desy.de/sites2009/site_vuvfel/content/e403/e1642/e164854/e164855/infoboxContent167617/TESLA-FEL2013-04.pdf